0026-895X/97/040613-10$3.00/0

MOLECULAR PHARMACOLOGY, **52:**613–622 (1997).

The Microtubule-Stabilizing Agent Discodermolide Competitively Inhibits the Binding of Paclitaxel (Taxol) to Tubulin Polymers, Enhances Tubulin Nucleation Reactions More Potently than Paclitaxel, and Inhibits the Growth of Paclitaxel-Resistant Cells

RICHARD J. KOWALSKI, PARASKEVI GIANNAKAKOU, SARATH P. GUNASEKERA, ROSS E. LONGLEY, BILLY W. DAY, and ERNEST HAMEL

Laboratory of Drug Discovery Research and Development, Developmental Therapeutics Program, Division of Cancer Treatment, Diagnosis, and Centers, National Cancer Institute, Frederick Cancer Research and Development Center, Frederick, Maryland 21702 (R.J.K., E.H.), Medicine Branch, Division of Clinical Sciences, National Cancer Institute, National Institutes of Health, Bethesda, Maryland 20892 (P.G.), Division of Biomedical Marine Research, Harbor Branch Oceanographic Institution, Fort Pierce, Florida 34946 (S.P.G., R.E.L.), and Department of Environmental and Occupational Health and Department of Pharmaceutical Sciences, University of Pittsburgh Cancer Institute, University of Pittsburgh, Pittsburgh, Pennsylvania 15238 (B.W.D.)

Received March 3, 1997; Accepted June 23, 1997

SUMMARY

The lactone-bearing polyhydroxylated alkatetraene (+)-discodermolide, which was isolated from the sponge *Discodermia dissoluta*, induces the polymerization of purified tubulin with and without microtubule-associated proteins or GTP, and the polymers formed are stable to cold and calcium. These effects are similar to those of paclitaxel (Taxol), but discodermolide is more potent. We confirmed that these properties represent hypernucleation phenomena; we obtained lower tubulin critical concentrations and shorter polymers with discodermolide than paclitaxel under a variety of reaction conditions. Furthermore, we demonstrated that discodermolide is a competitive inhibitor with [^{3}H]paclitaxel in binding to tubulin polymer, with an apparent K_i value of 0.4 μM. Multidrug-resistant human colon and ovarian carcinoma cells overexpressing P-glycoprotein, which are 900- and 2800-fold resistant to paclitaxel, respectively, relative to the parental lines, retained significant sensitivity to discodermolide (25- and 89-fold more resistant relative to the parental lines). Ovarian carcinoma cells that are 20–30-fold more resistant to paclitaxel than the parental line on the basis of expression of altered β-tubulin polypeptides retained nearly complete sensitivity to discodermolide. The effects of discodermolide on the reorganization of the microtubules of *Potorous tridactylis* kidney epithelial cells were examined at different times. Intracellular microtubules were reorganized into bundles in interphase cells much more rapidly after discodermolide treatment compared with paclitaxel treatment. A variety of spindle aberrations were observed after treatment with both drugs. The proportions of the different types of aberration were different for the two drugs and changed with the length of drug treatment.

Recently, an ever-increasing number of potently cytotoxic natural products that interact with tubulin have been isolated (see Ref. 1 for a review). Cells treated with these compounds arrest in the mitotic phase of the cell cycle. At medium-to-higher drug concentrations, this occurs because the microtubule spindle fails to form, whereas, at lower concentrations, these agents seem to interfere with spindle microtubule dynamics (2), apparently prolonging metaphase. Most of these antimitotic agents also cause the disappearance of intracellular microtubules. Such compounds invariably inhibit the assembly of microtubule protein or purified tubulin, often at concentrations substantially below the tubulin concentration in the reaction mixture.

A few antimitotic drugs, however, cause massive reorganization of intracellular microtubules and promote biochemical assembly reactions of both microtubule protein and purified tubulin. For more than 15 years, paclitaxel and structurally related taxoids were the only compounds known to have this mechanism of action (3). Recently, two additional drug classes have been shown to act by a similar mechanism. A computer-assisted search for novel compounds with structural analogy to colchicine site inhibitors suggested that the marine natural product (+)-discodermolide (4, 5), which was isolated from the sponge *Discodermia dissoluta*, could be an antimitotic agent (6), and initial studies with the compound had demonstrated potent antiproliferative activity (low

ABBREVIATIONS: MDR, multidrug resistant (resistance); MAP, microtubule-associated protein; MES, 2-(*N*-morpholino)ethanesulfonic acid; FCS, fetal calf serum; PBS, phosphate-buffered saline; PtK_2, *Potorous tridactylis* kidney epithelial.

nanomolar IC_{50} values), with cell cycle arrest at G2/M (7). However, the treatment of breast carcinoma cells with nanomolar concentrations of discodermolide resulted in spectacular microtubule bundle formation, even more extensive than that observed with micromolar concentrations of paclitaxel. Studies with purified tubulin confirmed that discodermolide was significantly more potent than paclitaxel in inducing polymerization under a variety of reaction conditions (8). The activity of epothilones A and B, isolated from the soil bacterium *Sorangium cellulosum*, was discovered through a screen of almost 8000 natural product extracts for compounds that would polymerize microtubule protein, and the purified compounds, like paclitaxel, caused extensive rearrangement of microtubules in cells (9). The structures of discodermolide and the epothilones are compared with that of paclitaxel in Fig. 1.

The diverse, seemingly unrelated, structures of these molecules raised the question of whether they bind to the same or different sites on tubulin. Radiolabeled taxoids seem to bind with high affinity only to polymerized forms of tubulin, and inhibitors of assembly usually simultaneously prevent paclitaxel-driven polymerization and binding of taxoid to tubulin (10–12). The epothilones (9, 13) and discodermolide (14, 15) were shown to inhibit the binding of [^{3}H]paclitaxel to tubulin polymers. Recently, we reported that epothilones A and B displayed kinetic inhibitory patterns observed with competitive inhibitors (13), indicating they bind to the paclitaxel site on polymer. A similar kinetic characterization of discodermolide binding was one of the goals of the current study, as was further characterization of the potent activity of discodermolide in nucleating microtubule assembly (8).

Paclitaxel and its semisynthetic analog docetaxel (Taxotere) have become increasingly important in the treatment of neoplastic diseases (16, 17), and it is to be hoped that discodermolide and the epothilones will have similar value. Paclitaxel is a substrate for P-glycoprotein, whose overexpression can be responsible for the MDR phenomenon. Epothilones A and B do not seem to bind to P-glycoprotein; a number of MDR cell lines that have lost their sensitivity to paclitaxel retain nearly complete sensitivity to both epothilones (9, 13, 18, 19). In addition, we found that the paclitaxel-resistant ovarian carcinoma cell lines 1A9PTX10 and 1A9PTX22, which express altered β-tubulins[1] (20), retained full sensitivity to epothilone B, whereas only 1A9PTX22 cells retained full sensitivity to epothilone A (13, 19). We evaluated the activity of discodermolide in two MDR carcinoma cell lines and in the paclitaxel-resistant 1A9PTX10 and 1A9PTX22 ovarian carcinoma lines. Further, microtubule bundles appear more rapidly in cells treated with discodermolide than in cells treated with paclitaxel. This complements the earlier observation that bundles appear after treatment of cells with significantly lower concentrations of discodermolide than of paclitaxel (8).

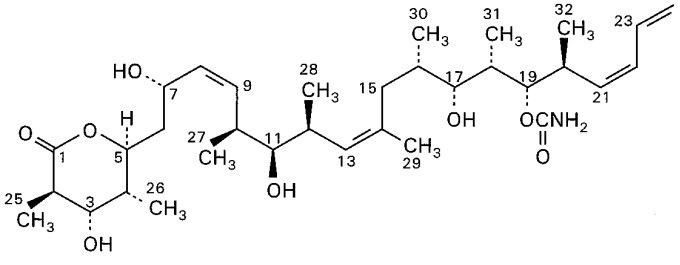

Discodermolide

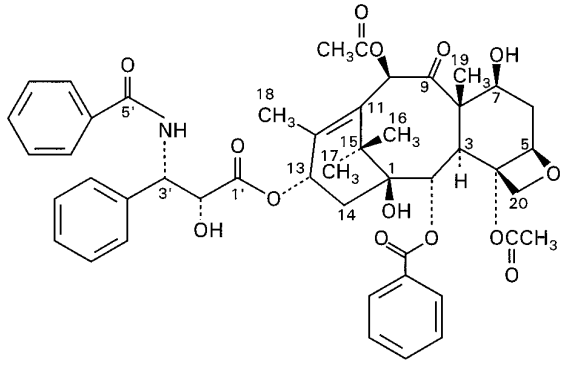

Paclitaxel

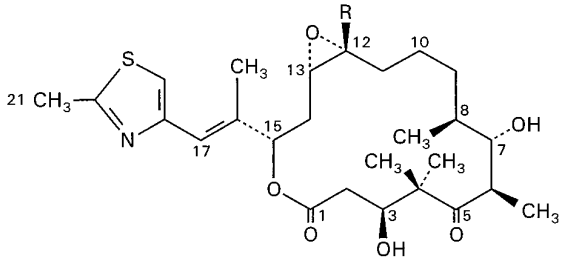

Epothilone A: R = H
Epothilone B: R = CH_3

Fig. 1. Structures of (+)-discodermolide, paclitaxel, and epothilones A and B. The configurations of the chiral centers of discodermolide are those shown in Ref. 38. The configurations of the chiral centers of epothilones A and B are those shown in Ref. 39.

Experimental Procedures

Materials. Discodermolide was isolated from *D. dissoluta* as previously described (21). Paclitaxel and [^{3}H]paclitaxel (19–23 mCi/mmol) were generously provided by the Drug Synthesis and Chemistry Branch, National Cancer Institute (Rockville, MD). Drugs were dissolved in dimethylsulfoxide, and control samples contained solvent equivalent to that in drug-treated cultures or reaction mixtures. Electrophoretically homogenous tubulin and heat-treated MAPs were prepared from bovine brain (22). Tubulin was freed from unbound nucleotide by gel filtration chromatography and reconcentrated as previously described (23). For the polymerization studies, 1.0 M glutamate (used to stabilize the tubulin; can replace MAPs in inducing tubulin assembly) was removed through dialysis against 0.1 M MES, pH 6.9. The tubulin was centrifuged to remove aggregated protein and stored in liquid nitrogen in 0.2-ml aliquots. PtK_2 cells were from American Type Culture Collection (Rockville, MD). The ovarian carcinoma line 1A9, a clone of line A2780 (24), was used to generate paclitaxel-resistant lines by incubating the cells with increasing concentrations of paclitaxel in the presence of verapamil (20). The ovarian MDR line A2780AD was also derived from line A2780 (25). The colon carcinoma line SW620 and its subline SW620AD-300, which overexpresses P-glycoprotein, have been previously described (26). Culture media and FCS were from GIBCO

[1] Both paclitaxel-resistant lines bear mutations in the M40 gene and express large amounts of its product, the β_I-tubulin isotype. In 1A9PTX10 the mutation is at residue 270 (phenylalanine to valine; TTT to GTT) and in 1A9PTX22 at residue 364 (alanine to threonine; GCA to ACA).

BRL (Gaithersburg, MD), Permanox and glass slides were from Nunc (Naperville, CT), and murine monoclonal anti-β-tubulin antibody and GTP were from Sigma Chemical (St. Louis, MO). GTP and ddGTP (from Pharmacia, Piscataway, NJ) were repurified by anion exchange chromatography on DEAE-cellulose. Texas Red-conjugated goat-antimouse IgG and ProLong antifade fluorescent mounting medium were from Molecular Probes (Eugene, OR). Epothilones A and B were generously provided by Merck Research Laboratories (Rahway, NJ).

Inhibition of human colon and human ovarian carcinoma cell growth. Cells were continuously incubated in RPMI medium containing 10% FCS, 12 μg/ml gentamicin sulfate, and 2 mM glutamine. The medium for the paclitaxel-resistant ovarian cells also contained 5 μg/ml verapamil (to inhibit expression of P-glycoprotein) and 15 ng/ml paclitaxel. Before drug treatment, the paclitaxel-resistant ovarian cells were removed from paclitaxel containing medium for 5–7 days. Drug effects were determined in 96-well microtiter plates, with cells fixed and stained for protein (27).

Indirect immunofluorescence. Confluent monolayers of PtK_2 cells, grown on 25-cm^2 plates, were suspended by incubation with 7 ml/plate of 0.05% trypsin and 0.53 mM EDTA in Hanks' balanced salt solution. Suspended cells were diluted 1:40 with minimal essential medium containing 1 mM sodium pyruvate, 0.1 mM nonessential amino acids, 10% FCS, 2 mM glutamine, and 10 μg/ml gentamicin sulfate and allowed to attach and grow for 24 hr at 37° in a humid 5% CO_2 atmosphere on sterile, eight-well Permanox or glass cell-culture slides (300 μl/well, 10^3 cells/well). Medium was removed, and attached cells were incubated in supplemented minimal essential medium containing 10 μM concentration of drug at 37°. After various incubation times, medium was removed, and cells were rinsed with 37° PBS. Attached cells were fixed in −20° methanol for 10 min, rinsed three times with PBS, and incubated in PBS containing 0.1% Triton X-100 and 10% FCS for 30 min at room temperature to block nonspecific antibody binding sites. The blocking buffer was removed, and the cells were incubated for 1 hr at 37° with antibody to β-tubulin (200 μl/well, 1:200 dilution blocking buffer). Cells were washed three times with PBS and incubated for 45 min with Texas Red-conjugated goat anti-mouse IgG (150 μl/well, 1:50 dilution in PBS). After removal of the secondary antibody by two washes with PBS, diaminopropidium iodide (2 μg/ml) dissolved in PBS was added to stain DNA. Slides were wet-mounted in ProLong according to the manufacturer's procedures. Images were obtained with a Nikon Optiphot-2 epifluorescence microscope. Photographs were taken directly from the stage with Kodak TRI-X PAN 400 or Kodak T-MAX 100 black-and-white film.

Inhibition of [^{3}H]paclitaxel binding to polymer. For all binding studies, tubulin polymer was preformed in the absence of drugs for 30 min at 37° in reaction mixtures containing 2 μM tubulin, 20 μM ddGTP, and 0.75 M monosodium glutamate (2 M stock solution adjusted to pH 6.6 with HCl). This condition induced nearly complete assembly of tubulin into polymer (data not presented; see Refs. 28–30). Mixtures of discodermolide with [^{3}H]paclitaxel in varying concentrations were added to preformed polymer and incubated for 30 min at 37°. Bound [^{3}H]paclitaxel was separated from free paclitaxel by centrifugation of the reaction mixtures at 14,000 rpm in an Eppendorf microfuge for 20 min at room temperature; >90% of added protein sedimented under these conditions, even in the absence of drug. Protein and radiolabel in both supernatants and pellets (dissolved in 0.1 M NaOH overnight and neutralized with 0.1 M HCl) were quantified according to the procedure of Lowry and liquid scintillation counting, respectively. Data from three independent experiments were combined for data analysis.

Tubulin assembly. Polymerization was followed turbidimetrically at 350 nm in Gilford (Oberlin, OH) model 250 spectrophotometers equipped with electronic temperature controllers. Base-line values were established with the reaction mixtures containing all components except drug held at 0° by the temperature controller. Drug (or an equivalent amount of dimethylsulfoxide) was added and mixed into the reaction mixture as quickly as possible, and the reaction was followed sequentially for ~10 min each at 0°, 10°, and 25° and for 20 min at 37°.

Electron microscopy. During polymerization reactions, 10-μl aliquots were removed at various times and placed onto 200-mesh carbon-coated, Formavar-treated copper grids. Samples were stained with several drops of 0.5% uranyl acetate and examined with a Zeiss model 10CA electron microscope.

Results

Competitive binding of discodermolide and paclitaxel to microtubules. We showed that discodermolide and paclitaxel caused Burkitt lymphoma cells to accumulate in mitotic arrest and led to rearrangement of the microtubule network of breast carcinoma cells. Both agents caused hypernucleation of tubulin polymerization in reactions with reduced requirements for GTP, MAPs, and higher incubation temperatures, and the polymers formed had increased stability to cold and calcium (8). These properties had been often described for paclitaxel (3, 12, 23, 31–34). Finally, discodermolide, like taxoids and the epothilones, inhibited the binding of [^{3}H]paclitaxel to tubulin polymer (14). In most respects, however, discodermolide seemed to be significantly more potent than paclitaxel, with more extensive reactions occurring at lower temperatures and drug concentrations (8), and discodermolide was particularly potent in inhibiting the binding of [^{3}H]paclitaxel to tubulin polymer (14). Hung *et al.* (15), using synthetic discodermolide, reported similar observations and also noted that paclitaxel only weakly inhibited the binding of [^{3}H]discodermolide to polymer.

The disparate structures of discodermolide and paclitaxel caused us to undertake studies to gain more specific information about their binding sites. Success in these experiments required that virtually all tubulin in the reactions be driven into polymer before the addition of [^{3}H]paclitaxel and inhibiting drugs. We accomplished this by using ddGTP to induce tubulin assembly (28–30). In the kinetic experiments summarized in Fig. 2, we demonstrated that discodermolide apparently is a competitive inhibitor of the binding of [^{3}H]paclitaxel to the polymer. (A similar finding, as a control experiment, was made with docetaxel, generously provided by Dr. D. G. I. Kingston.) Fig. 2A presents our binding data in the Hanes format, in which a competitive inhibitor generates a family of parallel curves at different inhibitor concentrations (35). Dixon analysis (35) of these data yielded an apparent K_i value of 0.4 μM for discodermolide (Fig. 2B); the value obtained for docetaxel was 0.3 μM.

Discodermolide nucleates microtubule assembly more potently than paclitaxel. Although many of the effects of paclitaxel on microtubule assembly (polymerization at low temperatures and without GTP and/or MAPs) probably are manifestations of the ability of paclitaxel to hypernucleate tubulin assembly, this property is directly demonstrated by the more extensive polymerization, shorter microtubules, and lower tubulin critical concentration observed with the drug. With paclitaxel analogs, we found excellent correlation of enhanced assembly effects with relative tubulin critical concentrations (23); we have now also found that among paclitaxel, docetaxel, and 2-debenzoyl-2-*meta*-azidobenzoylpaclitaxel, relative microtubule lengths decrease as taxoid potency increases. Paclitaxel is the least active among the three compounds and yields the longest

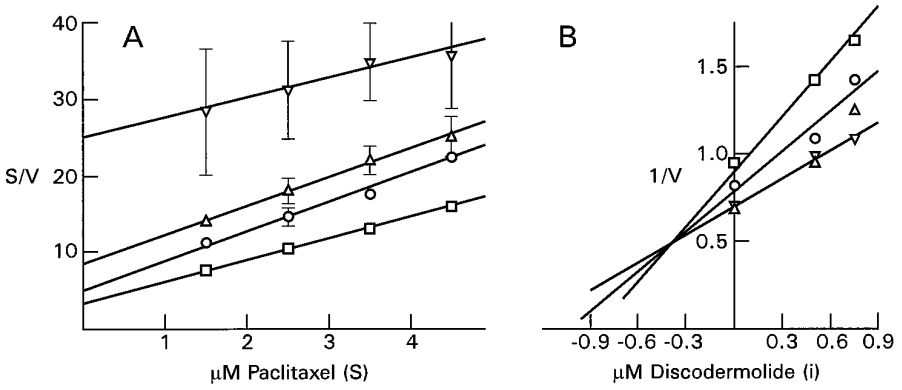

Fig. 2. Competitive inhibition of [^{3}H]paclitaxel binding to tubulin polymer by discodermolide. A, Hanes analysis. The reaction mixtures contained the components described in the text, together with the indicated concentrations of [^{3}H]paclitaxel and discodermolide at 0 (□), 0.5 (○), 0.75 (△), or 1.0 (▽) μM. See text for further details. The ordinate units are μM paclitaxel × pmol paclitaxel bound/μg of tubulin. B, Dixon analysis of the same data. The paclitaxel concentrations were 1.5 (□), 2.5 (○), 3.5 (△), or 4.5 (▽) μM. The ordinate units are pmol of paclitaxel bound/μg of tubulin. The data obtained with 3.5 μM paclitaxel were not used in determining the apparent K_i value.

microtubules, whereas 2-debenzoyl-2-*meta*-azidobenzoylpaclitaxel is the most active and yields the shortest microtubules.[2] Similarly, epothilone A had activity in inducing tubulin assembly and effects on tubulin critical concentration and microtubule lengths comparable to results obtained with paclitaxel, whereas epothilone B was distinctly more active (13).

In our initial studies with discodermolide (8), we found that its potency in inducing microtubule assembly reactions was significantly greater than that of paclitaxel. We have now determined the tubulin critical concentrations with discodermolide at 37° under a variety of reaction conditions in comparison with paclitaxel (Table 1). The experimental data were analyzed by linear regression to generate the values shown in Table 1. The turbidity values obtained below 1 μM tubulin were too low to be reliable (versus instrument noise). Several repetitions of experiments with 1 μM tubulin that yielded higher turbidity readings compared with reaction mixtures without drug convinced us that the critical concentrations for paclitaxel with MAPs plus GTP and for discodermolide with MAPs plus GTP, with MAPs only, and with GTP only were truly <1 μM.

With the tubulin and MAPs preparations used here, the tubulin critical concentration with 100 μM GTP was 3 μM (0.3 mg/ml). In previous experiments (23) without drug, MAPs or GTP, there was no assembly at tubulin concentrations up to 80 μM. With 10 μM paclitaxel, the tubulin critical concentration was <1 μM with both GTP and MAPs. The tubulin critical concentration increased to ~2 μM when GTP was not included in the reaction mixture, to ~4 μM without MAPs, and to ~20 μM without GTP and MAPs. This progressive increase in the critical concentration correlates well with the relative ability of tubulin to assemble with paclitaxel, particularly at low temperatures, under these different reaction conditions (8, 13, 23). With 10 μM discodermolide, the tubulin critical concentration was <1 μM under all reaction conditions except when neither GTP nor MAPs was in the reaction mixture, when a value of 3 μM was obtained. This was approximately one seventh of the value obtained with paclitaxel.

Polymer lengths were measured under all reaction conditions in which assembly occurred with 10 μM tubulin and 10 μM concentration of drug (Table 2). Data previously obtained (8) with both MAPs and GTP are also included in Table 2. In the MAPs-plus-GTP system, average polymer length without drug in both experiments was approximately twice that obtained with paclitaxel and 5–6-fold that obtained with discodermolide. With paclitaxel, there was a ~50% increase in average microtubule length with MAPs only and a 3-fold increase with GTP only compared with the complete system. With discodermolide, compared with the complete system, there was a ~50% increase in average length with MAPs only, a 2-fold increase with GTP only, and a 3-fold increase with neither MAPs nor GTP in the reaction.

Fig. 3 provides high-power views of the polymer formed with discodermolide under these four reaction conditions. With MAPs plus GTP (Fig. 3A), MAPs only (Fig. 3B), and no MAPs/no GTP (Fig. 3D), significant amounts of microtubule forms, mixed with ribbon polymers, were observed. With GTP only (Fig. 3C), most of the polymer was in the form of ribbons. The simultaneously obtained paclitaxel polymers were primarily of microtubule morphology (data not presented). Although the GTP-only sample with paclitaxel had a predominant microtubule morphology in the current study, we previously observed abundant ribbons under this reaction condition (23). The nuance in experimental conditions that results in this variability is not known.

Effects of discodermolide and paclitaxel on cultured human carcinoma cells. Table 3 summarizes the inhibitory effects of discodermolide and paclitaxel on the growth of several human tumor cell lines; these include two MDR lines to evaluate discodermolide as a potential substrate of P-

TABLE 1

Critical concentrations of tubulin for assembly with paclitaxel and discodermolide

Critical concentrations were measured in reaction mixtures containing 10 μM drug, 4% (v/v) dimethyl sulfoxide, 0.1 M MES (pH 6.9), and, if present, 100 μM GTP and MAPs at half the concentration (in mg/ml) of tubulin. Drug was the final addition to the reaction mixture. Critical concentrations were determined from final turbidity readings at 350 nm, with turbidity plotted against the tubulin concentration. The critical concentration was taken as the intercept on the concentration axis. Data are presented as concentration ± standard error of at least two independent experiments. For additional details, see Ref. 13. The data were analyzed by linear regression using the software program Origin (Microcal Software, Northampton, MA).

Drug	Critical concentration of tubulin			
	MAPs and GTP[a]	MAPs only	GTP only	No MAPs or GTP
	μM			
Paclitaxel	0.24 ± 0.3	1.7 ± 0.4	4.3 ± 0.4	22 ± 1
Discodermolide	0.41 ± 0.4	0.93 ± 0.2	0.88 ± 0.4	3.0 ± 0.3

[a] Without drug, the tubulin critical concentration under this reaction condition was 3.0 ± 0.05 μM.

[2] R. J. Kowalski and E. Hamel, unpublished observations.

TABLE 2

Microtubule lengths after assembly with paclitaxel and discodermolide

Electron micrographs were taken of samples from reaction mixtures containing 1.0 mg/ml (10 μM) tubulin, 10 μM concentration of drug, 4% (v/v) dimethyl sulfoxide, 0.1 M MES, pH 6.9, and, if present, 100 μM GTP and heat-treated MAPs at 0.5 mg/ml. Drug was the final addition to the reaction mixture. Reaction mixtures were incubated as described in Experimental Procedures. After 20 min at 37°, samples were applied to grids, which were used to prepare the micrographs used in the analyses presented in the table. Measurements were made on photographs at 4800× magnification for paclitaxel and without drug and 6000× for discodermolide. A minimum of 100 microtubules were measured for each reaction condition. Values are presented as mean ± standard deviation.

Drug	Average polymer length (relative to lengths with paclitaxel)			
	MAPs and GTP	MAPs only	GTP only	No MAPs or GTP
		μm		
None	4.3 ± 2 (2.3)			
	3.3 ± 2 (1.9)[a]			
Paclitaxel	1.9 ± 1 (1.0)	2.6 ± 1 (1.0)	6.0 ± 3 (1.0)	
	1.7 ± 0.6 (1.0)[a]			
Discodermolide	0.83 ± 0.4 (0.44)	1.2 ± 0.6 (0.46)	1.7 ± 1 (0.28)	2.3 ± 1.3
	0.58 ± 0.3 (0.34)[a]			

[a] Data from Ref. 8, a separate experiment.

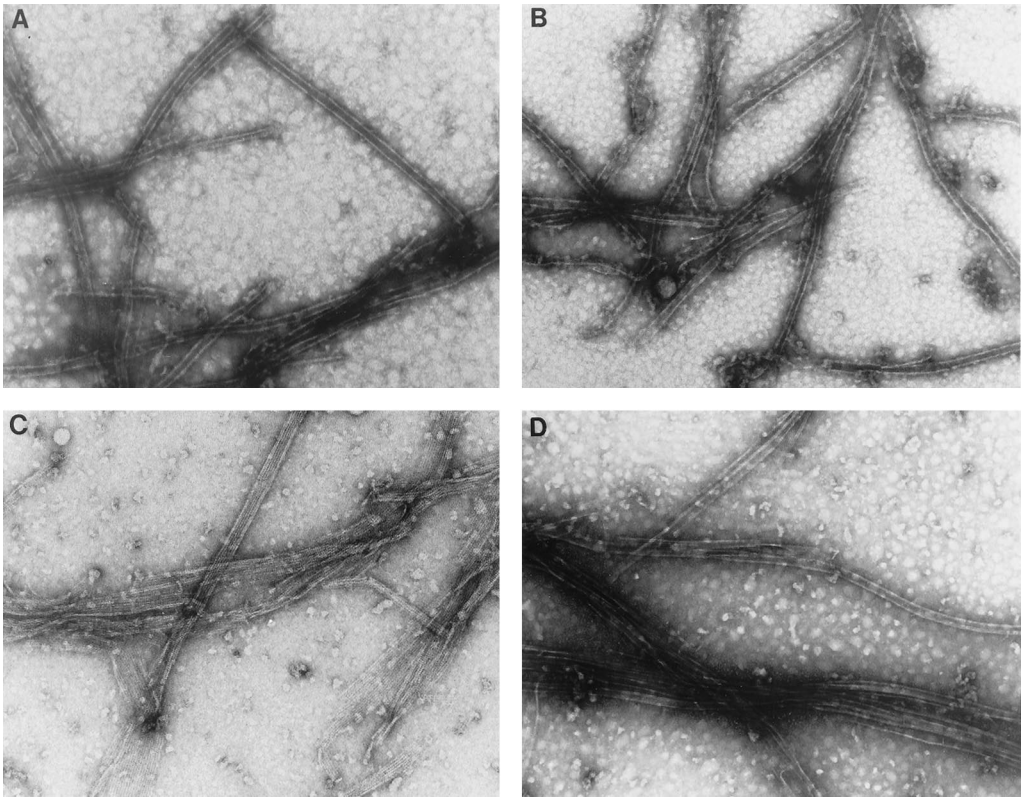

Fig. 3. Morphology of discodermolide-induced polymer. A, MAPs plus GTP. B, MAPs only. C, GTP only. D, No MAPs, no GTP. Magnifications, 49,000× (A, B, and D) and 63,000× (C). Reaction mixtures contained 10 μM tubulin, 10 μM discodermolide, 4% dimethylsulfoxide, 0.1 M MES, pH 6.9, and, if indicated, 100 μM GTP and 0.5 mg/ml heat-treated MAPs.

glycoprotein and two lines resistant to paclitaxel as a consequence of genetic alterations in a β-tubulin gene (20).

The parental colon carcinoma line SW620 was 10-fold more sensitive to paclitaxel than to discodermolide, but the MDR line derived from it was almost 4-fold more sensitive to discodermolide. The 930-fold increased resistance of the SW620AD-300 line to paclitaxel relative to the parental line was reduced to a 25-fold increased resistance to discodermolide. The parental ovarian line 1A9 was >4-fold less sensitive to discodermolide than to paclitaxel, but the related MDR line was almost 7-fold more sensitive to discodermolide. The 2800-fold increased resistance of the A2780AD line to paclitaxel relative to the 1A9 line was reduced to 89-fold increased resistance to discodermolide.

The ovarian lines 1A9PTX10 and 1A9PTX22 with altered β-tubulin gene products were >20-fold resistant to paclitaxel relative to the parental line. Both lines retained nearly complete sensitivity to discodermolide. As a consequence, these cells were significantly more sensitive to discodermolide than to paclitaxel.

Indirect immunofluorescence studies. Kangaroo rat PtK_2 cells were used to compare the effects of discodermolide with those of paclitaxel on intracellular microtubules (Figs. 4 and 5). IC_{50} values for this line, which were determined by counting both adherent and detached cells, were 250 and 120 nM for discodermolide and paclitaxel, respectively. To minimize concentration effects, cells were studied after treatment with 10 μM concentration of drug. We wanted to determine whether there was a difference in the time at which microtubule bundles appeared in drug-treated cells and to compare

TABLE 3

Inhibitory effects of paclitaxel and discodermolide on growth of human cancer cells

The colon carcinoma parental line is SW620, and the paclitaxel-resistant line is SW620AD-300, which overexpresses P-glycoprotein, resulting in MDR (26). The ovarian carcinoma parental line, designated 1A9, was derived as a subclone of line A2780 (24). The line A2780AD overexpresses P-glycoprotein (25). Two resistant lines, designated 1A9PTX10 and 1A9PTX22, were derived by growing the parental cells in paclitaxel and verapamil. Both lines express modified β-tubulin polypeptides (20). See footnote 1 in the text for further details. IC_{50} is the drug concentration that inhibits cell growth by 50%, as measured by cell protein. Relative resistance is obtained by dividing the IC_{50} value of the resistant line by the IC_{50} value of the parental line. Values are presented as mean ± standard error. The number of independent determinations in each case is indicated after the virgule.

	IC_{50} (relative resistance)					
	Colon carcinoma		Ovarian carcinoma			
	Parental	Pactitaxel resistant MDR	Parental	Paclitaxel resistant		
				MDR	β-tubulin mutants	
	SW620	SW620AD-300	1A9	A2780AD	1A9PTX10	1A9PTX22
				nM		
Paclitaxel	0.28 ± 0.08/2	260 ± 10/2 (930)	1.4 ± 0.2/11	3900 ± 400/4 (2800)	32 ± 8/7 (23)	41 ± 5/10 (29)
Discodermolide	2.8 ± 0.4/3	70 ± 10/3 (25)	6.5 ± 1/7	580 ± 200/3 (89)	7.2 ± 0.7/3 (1.1)	13 ± 3/6 (2.0)

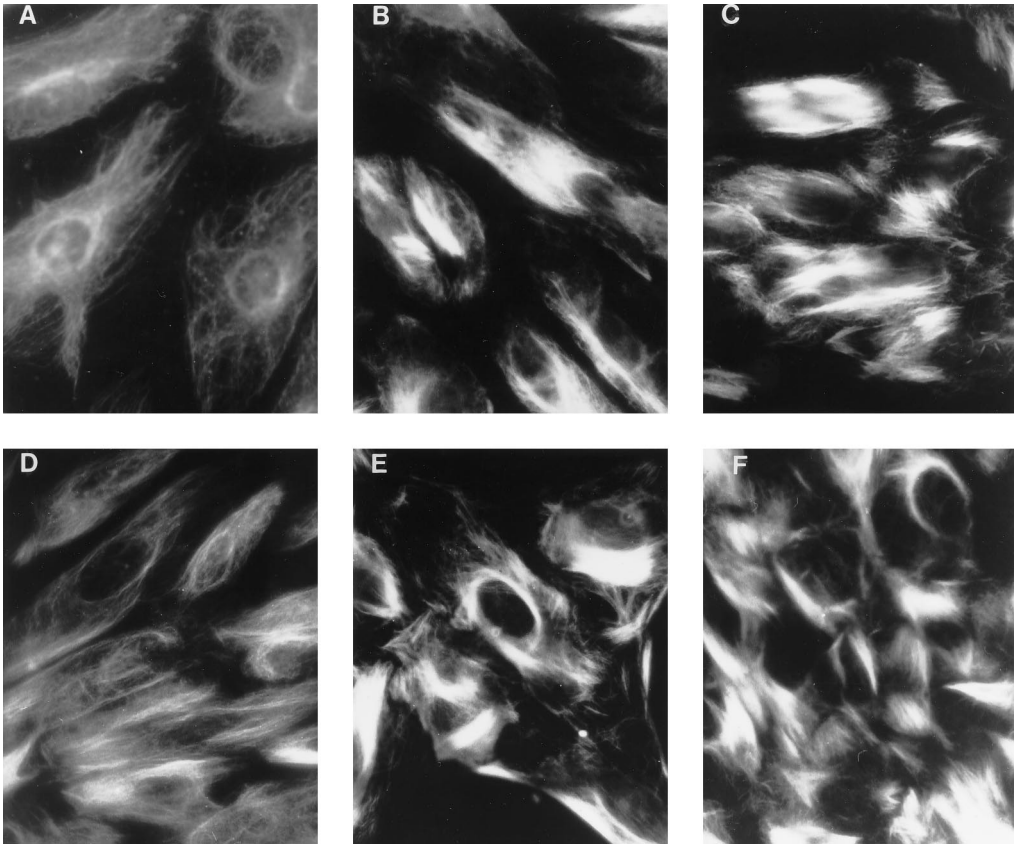

Fig. 4. Microtubule bundles form more rapidly in PtK_2 cells treated with discodermolide than with paclitaxel. A, No drug. B and C, Discodermolide. D–F, Paclitaxel. Cells were grown for 2 (A, B, and D), 6 (C and E), or 12 (F) hr at 37° before fixation and staining. See text for further details. Magnification, 630×.

the appearance of microtubules in mitotic cells after treatment with the two drugs. Cells were examined after drug treatment for 2, 6, 12, 24, and 48 hr.

Fig. 4 demonstrates that microtubule bundles appeared more rapidly after discodermolide treatment than after paclitaxel treatment, although both drugs ultimately caused microtubules in interphase cells to become nearly completely reorganized into bundles with multiple regions of nucleation. Fig. 4A illustrates the appearance of the rich microtubule network of untreated PtK_2 cells. After a 2-hr incubation in the presence of discodermolide (Fig. 4B), the microtubules in most cells were primarily found in thick bundles, and cells either had more than one microtubule organizing center or the microtubules arose independently of such centers. By 6 hr in discodermolide (Fig. 4C), this microtubule reorganization was complete, with no further changes at longer incubation times. With paclitaxel, there was relatively little microtubule reorganization into bundles after 2 hr (Fig. 4D), and even after 6 hr (Fig. 4E), microtubule bundling was incomplete. By 12 hr in paclitaxel (Fig. 4F), however, the appearance of interphase cells treated with the taxoid was indistinguishable from those treated with discodermolide.

Quantification of the mitotic index and mitotic aberrations was performed on cells incubated with drug for 2, 6, and 12 hr

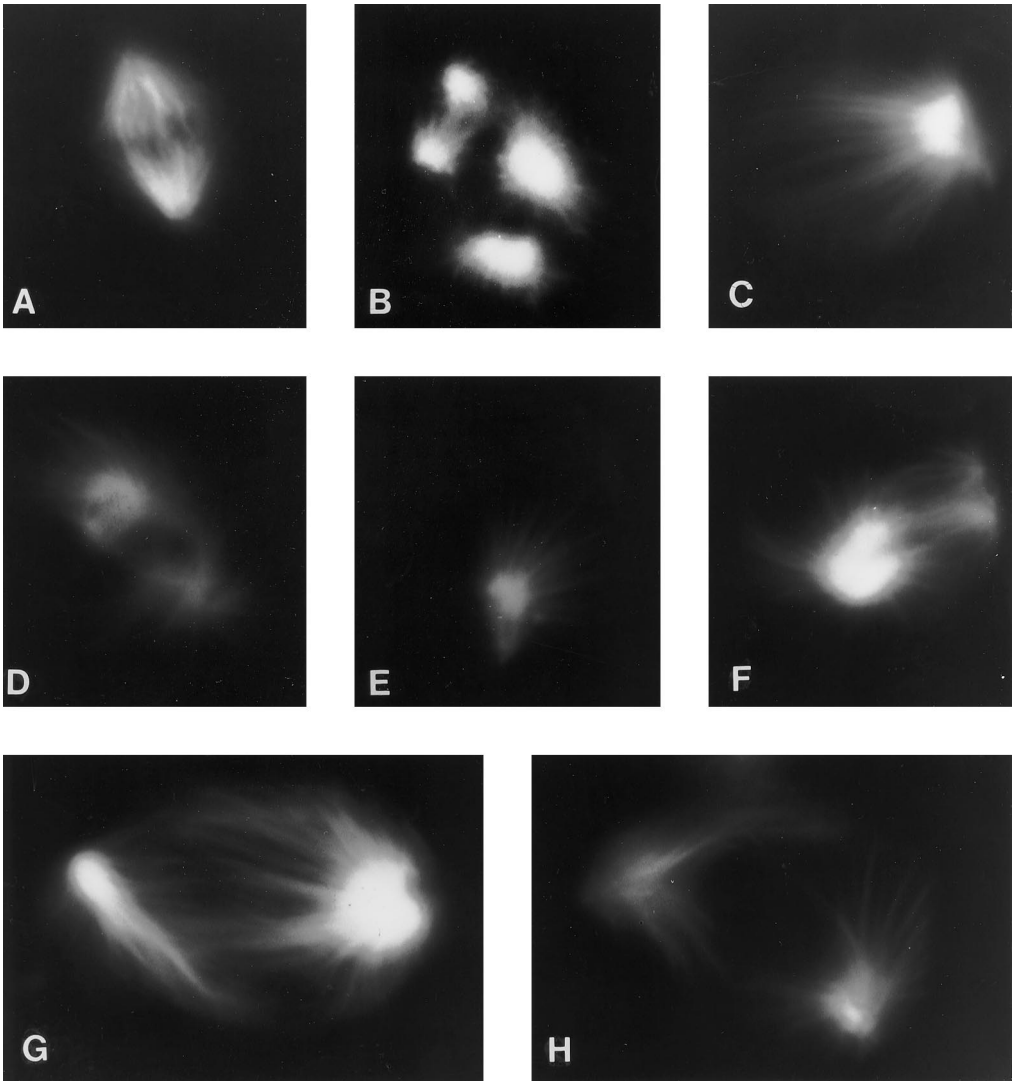

Fig. 5. Mitotic aberrations in PtK_2 cells after treatment with discodermolide. A, Control cell in metaphase (no drug) observed after growth for 6 hr. B, Aster spindle, observed after 2 hr in discodermolide. C and D, Spiral spindles, observed after 6 hr in discodermolide. E, Spike spindle, observed after 24 hr in discodermolide. F–H, Unclassified spindle aberrations, observed after 6 hr in discodermolide. See text for further details. All photographs were taken under oil with a 100× objective (numerical aperture, 1.30). Magnification, 1300×. Note that similar malformed spindles occur in paclitaxel-treated cells but in different proportions than in discodermolide-treated cells (see Table 4).

(Table 4). A control metaphase cell is shown in Fig. 5A, whereas aberrant mitotic figures after discodermolide treatment are shown in Fig. 5, B–H. Increased numbers of mitotic cells (those with condensed chromosomes and no nuclear membrane) were observed with both paclitaxel and discodermolide as early as 2 hr and, of the three time points examined, were maximal at 6 hr. All mitotic aberrations were present after treatment with both drugs, but their relative proportions varied between paclitaxel- and discodermolide-treated cells. Although the morphologies of the different types of aberrant "spindles" tended to blend into each other, making our classification scheme somewhat arbitrary, some mitotic aberrations occurred with sufficient frequency to permit the quantification of subtypes shown in Table 4. Paclitaxel produced more punctate-stained spindle aberrations, probably representing multiple microtubule organizing centers or spindle poles. Short filaments resembling astral microtubules were attached to the multiple spindle poles; these were called "aster spindles" (Fig. 5B but after discodermolide treatment). With discodermolide, the most common type of mitotic cell had a complex, spiral-like microtubule array, which is best appreciated by examining the cell at several focal planes. The microtubules in these cells were relatively long, and there was usually only one apparent or two poorly separated microtubule organizing centers. Such a "spiral spindle" is shown in Fig. 5C. Sometimes, however, the microtubule organizing centers were well separated, yielding a double spiral (Fig. 5D). Cells with spiral spindles, but in a lower proportion, were also observed after paclitaxel treatment. At 12 hr, a third type of mitotic aberration was ob-

TABLE 4

Mitotic index and aberrations induced by paclitaxel and discodermolide in PtK_2 cells

Cells were cultured, stained, and examined as described in detail in Experimental Procedures. The mitotic index is the percentage of examined cells judged to be mitotic by the presence of condensed chromosomes and no apparent nuclear membrane. An average of 236 cells were counted from each specimen (range, 155–265). The mitotic index of untreated cells was 1.5. The spindle percentages refer to the mitotic population only.

Drug	Incubation time	Mitotic index	Aster spindles	Spiral spindles	Spike spindles
	hours	*%*		*%*	
Paclitaxel	2	11	47	0	0
	6	23	67	2	0
	12	17	31	41	21
Discodermolide	2	8	21	37	0
	6	17	13	85	2
	12	17	11	68	21

served with both drugs ("spike spindles"). Cells with these structures had clusters of thick microtubule bundles, with the microtubules of intermediate length between those of the shorter aster spindle microtubules and the longer spiral spindle microtubules. In most cases, cells with spike spindles had one or two microtubule organizing centers (Fig. 5E). Separation between spike spindle microtubule organizing centers was highly variable. In addition, a significant number of mitotic cells could not be readily classified into one of these categories (Figs. 5, F–H). It is unknown whether there is any progression in these spindle variants or whether the proportions of specific spindle morphologies reflect different lengths of drug treatment relative to stage in the cell cycle for specific cells.

Discussion

Interaction of discodermolide with tubulin. The tubulin-based experiments were undertaken to determine whether the strong binding of discodermolide to tubulin polymers (8, 14, 15) occurred at the same site as paclitaxel binding and to confirm the hypothesis that the potent induction of tubulin assembly observed with discodermolide compared with paclitaxel represented superior activity in hypernucleating polymerization reactions.

With discodermolide, we obtained a competitive pattern of inhibition of binding of [^{3}H]paclitaxel to tubulin polymer (Fig. 2), and a similar pattern was obtained with the taxoid docetaxel. Classically, such results are interpreted as indicating that "substrate" (paclitaxel) and "inhibitor" (discodermolide) bind in the same site, but overlapping sites and/or allosteric effects cannot be readily eliminated as possible alternative explanations. The apparent K_i values obtained for discodermolide (0.4 μM) and docetaxel (0.3 μM) were essentially identical, even though discodermolide is the more potent compound in inducing tubulin assembly.

Both tubulin critical concentrations and polymer lengths were lower with discodermolide than with paclitaxel under every reaction condition examined in which reliable quantitative measurements could be made (Tables 1 and 2). Thus, with discodermolide, as with taxoids and the epothilones, polymer length data and tubulin critical concentrations support the concept that the reduced requirements for MAPs and GTP result from the ability of this broad class of drugs to hypernucleate tubulin assembly. The four systems we studied seem to have the following potency order for supporting nucleation: MAPs plus GTP > MAPs only > GTP only > no MAPs/no GTP.

The most reliable quantitative comparison between paclitaxel and discodermolide was probably the 7-fold-lower critical concentration obtained with discodermolide in the absence of both MAPs and GTP. This was in excellent agreement with another assay we performed to obtain a quantitative measure of the relative potency of the two drugs, in which we found that 3.2 μM discodermolide and 23 μM paclitaxel induced 50% tubulin assembly in 0.4 M glutamate without GTP (8), also a ~7-fold difference. The two measures together perhaps indicate the relative affinities of the two drugs for tubulin. Because no polymer exists in either 0.1 M MES or 0.4 M glutamate without GTP or MAPs, these relative affinities may apply to the α,β-heterodimer rather than to polymerized forms of tubulin, but transient polymeric forms that bind the drugs and are in turn stabilized by them cannot be excluded as an alternate explanation.

In summary, the biochemical analysis is most consistent with the two drugs acting by a similar mechanism of action, with discodermolide having a higher affinity than paclitaxel for tubulin (probably 5–10-fold greater).

Effects of discodermolide on cellular microtubule morphology. Previous work with breast carcinoma cells showed that discodermolide more potently induced microtubule bundle formation than did paclitaxel (8). Despite nearly equivalent IC_{50} values of the two drugs in the cell lines studied, bundle formation observed with 10 nM discodermolide required 1 μM paclitaxel. Few mitotic cells were observed in the breast carcinoma cultures, but both interphase and mitotic Swiss 3T3 cells were reported to have multiple bundles of microtubules after discodermolide treatment (15). In our study with PtK_2 cells (Fig. 4), we found that microtubule bundling occurred much more rapidly with discodermolide than with paclitaxel treatment, but that after 12 hr, the appearance of interphase cells treated with the two drugs was identical. We also observed that mitotic PtK_2 cells (no nucleus; condensed chromosomes) differed dramatically in appearance from interphase cells (with nuclei) after treatment with the two drugs. A variety of microtubule patterns was observed in the mitotic cells, and their distribution changed as a function of incubation time in the presence of drug (Table 4, Fig. 5). Precise proportions of different aberrant spindles differed with the two drugs and changed over time, but we could detect no discodermolide- or paclitaxel-specific spindle variant.

The enhanced bundling observed with discodermolide compared with paclitaxel is readily understood in terms of the apparent increased affinity of discodermolide for tubulin relative to paclitaxel. The differences in the proportions of mitotic aberrations seen with the two drugs and, indeed, the changing distribution of these aberrations as a function of time are not readily explained by the biochemical properties we examined. However, it seems probable that paclitaxel and discodermolide will differ either quantitatively or qualitatively in their effects on microtubule dynamics, and dynamic effects may be more important in mitotic cells than in interphase cells (36, 37). We should also note that the differing mitotic aberrations may also ultimately derive from relative affinities for tubulin. Epothilone B has a higher affinity for tubulin than epothilone A on the basis of apparent K_i values for inhibition of paclitaxel binding to polymer and its more potent enhancement of nucleation. After epothilone B treatment, PtK_2 cells had large numbers of spiral spindles, whereas after epothilone A treatment, aster spindles were more prevalent (13). Thus, comparable distributions of mitotic aberrations were observed with the more potent agents (discodermolide and epothilone B), on the one hand, and with the less potent agents (paclitaxel and epothilone A), on the other. In support of this idea, the morphological effects of these four agents on the PtK_2 cells was more closely related to their apparent affinities for tubulin (discodermolide > epothilone B > epothilone A ~ paclitaxel) than on their effects on growth of the cell line [epothilone A ~ epothilone B > paclitaxel > discodermolide (40, 44, 120, and 250 nM IC_{50} values, respectively)].

Effects of discodermolide on the growth of paclitaxel-resistant human cancer cell lines. The most notable differ-

ences observed between discodermolide and paclitaxel occurred with the paclitaxel-resistant human carcinoma cells (Table 3). We evaluated two MDR lines strongly resistant to paclitaxel (the colon line expresses a lower level of P-glycoprotein than the ovarian line, accounting for its greater sensitivity to paclitaxel) and two lines with moderate resistance on the basis of expression of two different altered β-tubulin polypeptides.

Both MDR lines retained some sensitivity to discodermolide in that the relative resistance factors were 30–40-fold lower than those obtained with paclitaxel. This suggests that discodermolide has a reduced affinity for P-glycoprotein relative to paclitaxel, but this will need to be confirmed with additional MDR lines. In comparison, epothilones A and B seem to have negligible affinity for P-glycoprotein in all MDR lines thus far examined (9, 13, 18, 19).

The ovarian lines 1A9PTX10 and 1A9PTX22 express high levels of altered β_I-tubulin isotypes. The changes occur in the primary sequence of the polypeptide chain at positions 270 for 1A9PTX10 (phenylalanine to valine) and 364 for 1A9PTX22 (alanine to threonine) (20). The two cell lines show a 25–30-fold increased resistance to paclitaxel, and both lines retain nearly complete sensitivity to discodermolide. Because the alterations in β-tubulin associated with decreased sensitivity to paclitaxel probably derive from a decreased affinity of paclitaxel for tubulin or tubulin polymers (20), the affinity of the altered tubulin for discodermolide is probably little changed. This finding differs from the relative resistance obtained with epothilone derivatives; for of six compounds examined thus far in both cell lines (19, 20), only epothilone B was fully active. Epothilone A, an epothilone B analog that had effects on tubulin polymerization equivalent to those of epothilone B, and three additional derivatives retained nearly full activity in the 1A9PTX22 line (resistance factors of 1.6–3.0) but were relatively inactive in the 1A9PTX10 line (resistance factors of 8.6–17). These observations may indicate subtle differences in the amino acid residues that form the drug binding site with each class of drug, and, specifically, that discodermolide interacts minimally with both Phe270 and Ala364.

The higher affinity of discodermolide for tubulin, the differences in its effects from paclitaxel on cultured cells, and its probable greater aqueous solubility (8) all argue for its careful evaluation as an anticancer drug. The recent synthesis of discodermolide (38) increases the feasibility of such an evaluation.

References

1. Hamel, E. Antimitotic natural products and their interactions with tubulin. *Med. Res. Rev.* **16:**207–231 (1996).
2. Wilson, L., and M. A. Jordan. Microtubule dynamics: taking aim at a moving target. *Chem. Biol.* **2:**569–573 (1995).
3. Schiff, P. B., J. Fant, and S. B. Horwitz. Promotion of microtubule assembly in vitro by taxol. *Nature (Lond.)* **277:**665–667 (1979).
4. Gunasekera, M., S. P. Gunasekera, R. E. Longley, and N. S. Burres, inventors. Harbor Branch Oceanographic Institution, assignee. U.S. Patent 4,939,168 (1990).
5. Gunasekera, M., S. P. Gunasekera, R. E. Longley, and N. S. Burres, inventors. Harbor Branch Oceanographic Institution, assignee. U.S. Patent 5,010,099 (1991)
6. ter Haar, E., H. S. Rosenkranz, E. Hamel, and B. W. Day. Computational and molecular modeling evaluation of the structural basis for tubulin polymerization inhibition by colchicine site agents. *Bioorg. Med. Chem.* **4:**1659–1671 (1996).
7. Longley, R. E., S. P. Gunasekera, D. Faherty, J. McLane, and F. Dumont. Immunosuppression by discodermolide. *Ann. N. Y. Acad. Sci.* **696:**94–107 (1993).
8. ter Haar, E., R. J. Kowalski, E. Hamel, C. M. Lin, R. E. Longley, S. P. Gunasekera, H. S. Rosenkranz, and B. W. Day. Discodermolide, a cytotoxic marine agent that stabilizes microtubules more potently than taxol. *Biochemistry* **35:**243–250 (1996).
9. Bollag, D. M., P. A. McQueney, J. Zhu, O. Hensens, L. Koupal, J. Liesch, M. Goetz, E. Lazarides, and C. M. Woods. Epothilones, a new class of microtubule-stabilizing agents with a taxol-like mechanism of action. *Cancer Res.* **55:**2325–2333 (1995).
10. Parness, J., and S. B. Horwitz. Taxol binds to polymerized tubulin in vitro. *J. Cell Biol.* **91:**479–487 (1981).
11. Takoudju, M., M. Wright, J. Chenu, F. Guéritte-Voegelein, and D. Guénard. Absence of 7-acetyl taxol binding to unassembled brain tubulin. *FEBS Lett.* **227:**96–98 (1988).
12. Díaz, J. F., and J. M. Andreu. Assembly of purified GDP-tubulin into microtubules induced by taxol and taxotere: reversibility, ligand stoichiometry, and competition. *Biochemistry* **32:**2747–2755 (1993).
13. Kowalski, R. J., P. Giannakakou, and E. Hamel. Activities of the microtubule-stabilizing agents epothilones A and B with purified tubulin and in cells resistant to paclitaxel (Taxol®). *J. Biol. Chem.* **272:**2534–2541 (1997).
14. Kowalski, R. J., E. ter Haar, R. E. Longley, S. P. Gunasekera, C. M. Lin, B. W. Day, and E. Hamel. Comparison of novel microtubule polymerizing agents, discodermolide and epothilone A/B, with taxol. *Mol. Biol. Cell* **6:**368a (1995).
15. Hung, D. T., J. Chen, and S. L. Schreiber. (+)-Discodermolide binds to microtubules in stoichiometric ratio to tubulin dimers, blocks taxol binding and results in mitotic arrest. *Chem. Biol.* **3:**287–293 (1996).
16. Rowinsky, E. K., and R. C. Donehower. Paclitaxel (Taxol). *N. Engl. J. Med.* **332:**1004–1014 (1995).
17. Cortes, J. E., and R. Pazdur. Docetaxel. *J. Clin. Oncol.* **13:**2643–2655 (1995).
18. Su, D.-S., D. Meng, P. Bertinato, A. Balog, E. J. Sorenen, S. J. Danishefsky, Y.-H. Zheng, and T.-C. Chou. Total synthesis of (−)-epothilone B: an extension of the Suzuki coupling method and insights into structure-activity relationships of the epothilones. *Angew. Chem. Int. Ed. Engl.* **36:**757–760 (1997).
19. Nicolaou, K. C., N. Winssinger, J. Pastor, S. Ninkovic, F. Sarabia, Y. He, D. Vourloumis, Z. Yang, T. Li, P. Giannakakou, and E. Hamel. Synthesis of epothilones A and B in solid and solution phase. *Nature (Lond.)* **387:** 268–272 (1997).
20. Giannakakou, P., D. L. Sackett, Y.-K. Kang, Z. Zhan, J. T. M. Buters, T. Fojo, and M. S. Poruchynsky. Paclitaxel resistant human ovarian cancer cells have mutant β-tubulins that exhibit impaired paclitaxel driven polymerization. *J. Biol. Chem.* **272:**17118–17125 (1997).
21. Gunasekera, S. P., M. Gunasekera, R. E. Longley, and G. K. Schulte. Discodermolide: a new bioactive polyhydroxylated lactone from the marine sponge *Discodermia dissoluta*. *J. Org. Chem.* **55:**4912–4915 (1991) [published erratum appears in *J. Org. Chem.* **56:**1346 (1991)].
22. Hamel, E., and C. M. Lin. Separation of active tubulin and microtubule-associated proteins by ultracentrifugation and isolation of a component causing the formation of microtubule bundles. *Biochemistry* **23:**4173–4184 (1984).
23. Grover, S., J. R. Rimoldi, A. A. Molinero, A. G. Chaudhary, D. G. I. Kingston, and E. Hamel. Differential effects of paclitaxel (Taxol) analogs modified at positions C-2, C-7, and C-3′ on tubulin polymerization and polymer stabilization: identification of a hyperactive paclitaxel derivative. *Biochemistry* **34:**3927–3934 (1995).
24. Behrens, B. C., T. C. Hamilton, H. Masuda, K. R. Grotzinger, J. Whang-Peng, K. G. Louie, T. Knutsen, W. M. McKoy, R. C. Young, and R. F. Ozols. Characterization of a *cis*-diamminedichloroplatinum(II)-resistant human ovarian cancer cell line and its use in evaluation of platinum analogues. *Cancer Res.* **47:**414–418 (1987).
25. Rogan, A. M., T. C. Hamilton, R. C. Young, R. W. Klecker, Jr., and R. Ozols. Reversal of adriamycin resistance by verapamil in human ovarian cancer. *Science (Washington D. C.)* **244:**994–996 (1984).
26. Lai, G. M., Y.-N. Chen, L. A. Mickley, A. T. Fojo, and S. E. Bates. P-glycoprotein expression and schedule dependence of adriamycin toxicity in human carcinoma cell lines. *Int. J. Cancer* **49:**696–703 (1991).
27. Skehan, P., R. Storeng, D. Scudiero, A. Monks, J. McMahon, D. Vistica, J. T. Warren, H. Bokesch, S. Kenney, and M. R. Boyd. New colorimetric cytotoxicity assay for anticancer-drug screening. *J. Natl. Cancer Inst.* **82:**1107–1112 (1990).
28. Hamel, E., A. A. del Campo, and C. M. Lin. Stability of tubulin polymers formed with dideoxyguanosine nucleotides in the presence and absence of microtubule-associated proteins. *J. Biol. Chem.* **259:**2501–2508 (1984).
29. Hamel, E., J. Lustbader, and C. M. Lin. Deoxyguanosine nucleotide analogues: potent stimulators of microtubule nucleation with reduced affinity for the exchangeable nucleotide site of tubulin. *Biochemistry* **23:**5314–5325 (1984).
30. Hamel, E., J. Vaughns, Z. Getahun, and C. M. Lin. Interactions of tubulin with guanine nucleotides that have paclitaxel-like effects on tubulin assembly: 2′,3′-dideoxyguanosine 5′-[α,β-methylene]triphosphate, guanosine 5′-[α,β-methylene]triphosphate, and 2′,3′,-dideoxyguanosine 5′-triphosphate. *Arch. Biochem. Biophys.* **322:**486–499 (1995).
31. Hamel, E., A. A. del Campo, M. C. Lowe, and C. M. Lin. Interactions of taxol, microtubule-associated proteins, and guanine nucleotides in tubulin polymerization. *J. Biol. Chem.* **256:**11887–11894 (1981).

32. Kumar, N. Taxol-induced polymerization of purified tubulin: mechanism of action. *J. Biol. Chem.* **256:**10435–10441 (1981).
33. Schiff, P. B., and S. B. Horwitz. Taxol assembles tubulin in the absence of exogenous guanosine 5′-triphosphate or microtubule-associated proteins. *Biochemistry* **20:**3247–3252 (1981).
34. Thompson, W. C., L. Wilson, and D. L. Purich. Taxol induces microtubule assembly at low temperature. *Cell Motil.* **1:**445–454 (1981).
35. Dixon, M., E. C. Webb, C. J. R. Thorne, and K. F. Tipton. *Enzymes.* Academic Press, New York (1979).
36. Jordan, M. A., R. J. Toso, D. Thrower, and L. Wilson. Mechanism of mitotic block and inhibition of cell proliferation of taxol at low concentrations. *Proc. Natl. Acad. Sci. USA* **90:**9552–9556 (1993).
37. Derry, W. B., L. Wilson, and M. A. Jordan. Substoichiometric binding of taxol suppresses microtubule dynamics. *Biochemistry* **34:**2203–2211 (1995).
38. Hung, D. T., J. B. Nerenberg, and S. L. Schreiber. Syntheses of discodermolides useful for investigating microtubule binding and stabilization. *J. Am. Chem. Soc.* **118:**11054–11080 (1996).
39. Höfle, G., N. Bedorf, H. Steinmetz, D. Schomberg, K. Gerth, H. Reichenbach. Epothilone A and B — novel 16-membered macrolides with cytotoxic activity: isolation, crystal structure, and conformation in solution. *Angew. Chem. Int. Ed. Engl.* **35:**1567–1569 (1996).

Send reprint requests to: Dr. Ernest Hamel, NIH, Building 37, Rm. 5C25, 37 Convent Drive, MSC 4255, Bethesda, MD 20892-4255.